01 Jan 1991

Electrical Conductivity, Seebeck Coefficient And Defect Chemistry Of Ca-doped YCrO3

G. F. Carini

Harlan U. Anderson
Missouri University of Science and Technology, harlanua@mst.edu

Don M. Sparlin
Missouri University of Science and Technology, sparlin@mst.edu

M. M. Nasrallah

Recommended Citation

G. F. Carini et al., "Electrical Conductivity, Seebeck Coefficient And Defect Chemistry Of Ca-doped YCrO3," *Solid State Ionics*, vol. 49, pp. 233 - 243, Elsevier, Jan 1991.
The definitive version is available at https://doi.org/10.1016/0167-2738(91)90091-O

Solid State Ionics 49 (1991) 233–243
North-Holland

SOLID
STATE
IONICS

Electrical conductivity, Seebeck coefficient and defect chemistry of Ca-doped $YCrO_3$

G.F. Carini II, H.U. Anderson, D.M. Sparlin and M.M. Nasrallah
Ceramic Engineering Department, University of Missouri-Rolla, Rolla, MO 65401, USA

The electrical transport behavior and defect structure of Ca-doped $YCrO_3$ were studied using electrical conductivity and Seebeck coefficient measurements as a function of oxygen activity and temperature. Defect models derived from the electrical conductivity data were found to adequately relate the concentration of charge carriers to the acceptor dopant and oxygen vacancy concentrations. Thermodynamic properties were calculated and found to be consistent with the model. Activation energy and carrier mobility data were also obtained. The analysis of the electrical conductivity, Seebeck and mobility data suggest that the conduction process in Ca-doped $YCrO_3$ occurs via the small polaron hopping mechanism.

1. Introduction

Since the advent of the first solid oxide fuel cells there has been a continuous effort to improve the electrical and physicochemical properties of the cell electrodes and interconnects [1]. These factors are crucial in determining a fuel cell's usefulness as a power generator. Acceptor doped refractory perovskites such as (La, Sr, Mg) (Cr, Mn)O_3 have shown some promise. However, problems such as hydration [2,3] or volatilization [4,5] of Cr oxides are known to diminish the efficiency and longevity. For this reason, alternative materials with a greater stability in corrosive environments need to be developed. One possible option is $YCrO_3$. It is isostructural with $LaCrO_3$ and possesses similar electrical and thermal characteristics [6–10]. Published works regarding the electrical behavior with respect to oxygen activity of $YCrO_3$-based ceramics are virtually nonexistent. The purpose of this study was to define the effects of acceptor dopants on the redox behavior and defect structure of $YCrO_3$. The electrical conductivity and Seebeck coefficient as a function of oxygen activity were determined experimentally. A defect model was developed and related to the data. An electrical transport mechanism was proposed.

2. Proposed defect model

Prior to this investigation, documentation concerning the defect structure of (Y, Ca)CrO_3 was limited. However, $LaCrO_3$ has been extensively studied and, due to their identical structure, it is expected that both systems will exhibit similar electrical behavior in reducing conditions. Anderson et al. [11], proposed a defect model for acceptor doped $LaCrO_3$ which successfully predicted the stability of the electrical conductivity and defect structure for various regions of oxygen activity and temperature. This method was also found to be appropriate for characterizing other systems including (La, Sr)MnO_3 [12], La(Mn, Mg)O_3 [13], and Li-doped Cr_2O_3 [14]. For the (Y, Ca)CrO_3 system, a defect model analogous to the one suggested by Anderson et al. will be adopted. It is assumed that the formation of oxygen vacancies would occur at low oxygen activities and that the acceptors are then compensated by the oxygen vacancies rather than by Cr^{4+}. A reaction of this nature could be written as (using Kröger–Vink notation [15]):

$$Y_{1-x}Ca'_xCr^{\times}_{1-x}Cr^{\cdot}_xO_3 \rightleftharpoons Y_{1-x}Ca'_xCr^{\times}_{1-x+2y}Cr^{\cdot}_{x-2y}(V^{\cdot\cdot}_O)_yO_{3-y}+y/2O_2\,, \quad (1)$$

where $(V^{\cdot\cdot}_O)$ represents oxygen vacancies with an ef-

fective charge of +2. In terms of reactants and products only, eq. (1) can be simplified to

$$O_O + 2Cr_{Cr}^{\cdot} = 2Cr_{Cr}^{\times} + V_O^{\cdot\cdot} + \tfrac{1}{2}O_2 . \quad (2)$$

If the defects are assumed to be randomly distributed and noninteractive, the Law of Mass Action gives the equilibrium constant for eq. (2) as

$$K = (a^2_{Cr_{Cr}^{\times}} a_{(V_O^{\cdot\cdot})} a^{1/2}_{O_2}) / (a_{O_O} a^2_{Cr_{Cr}^{\cdot}}) , \quad (3)$$

where $a_{Cr_{Cr}^{\times}}$, $a_{V_O^{\cdot\cdot}}$, a_{O_2}, and $a_{Cr_{Cr}^{\cdot}}$ are the activities of the respective structure elements, and K is the equilibrium constant. If it is assumed that the activities of the various species can be approximated by their concentrations as mole fractions, then eq. (3) becomes

$$K = [(1-x+2y)^2 y P^{1/2}_{O_2}] / (x-2y)^2 , \quad (4)$$

where x is the Ca concentration, y is the oxygen vacancy concentration, and P_{O_2} is the oxygen partial pressure. Since both x and y are small compared to 1, eq. (4) can be approximated by

$$K = (y P^{1/2}_{O_2}) / (x-2y)^2 . \quad (5)$$

This expression yields a quadratic equation which can be solved and rearranged to give an expression relating the oxygen activity and x to $(V_O^{\cdot\cdot})$, accordingly

$$2y = x - (P^{1/2}_{O_2}/4K)[(8xKP^{-1/2}_{O_2} + 1)^{1/2} - 1] . \quad (6)$$

This expression gives $y=0$ at high oxygen activities. At low oxygen activities, eq. (6) yields a limiting expression of

$$(x-y)/x = P^{1/4}_{O_2} / (2xK)^{1/2} . \quad (7)$$

An extension of this model can be applied to predict the behavior of the electrical conductivity. For this case it is assumed that the small polaron hopping transport is dominant and that the formation of oxygen vacancies directly compensates the acceptors thereby decreasing the conductivity. This assumption is reasonable provided that there are no significant changes in the carrier mobility. Thus, the conductivity of (Y, Ca)CrO_3 is expected to remain constant throughout the high P_{O_2} region, and to decrease proportionally to the amount of liberated O_2 at low P_{O_2}. If it is assumed that the conductivity is independent of any scattering or trapping effects, then the previous relation between $V_O^{\cdot\cdot}$ and P_{O_2} can be used to calculate the relation between conductivity and P_{O_2}. The electrical conductivity will be directly proportional to the product of the carrier concentration and mobility, as represented by

$$\sigma = e\mu p , \quad (8)$$

where σ is the electrical conductivity, e is the charge of an electron, p is the concentration of holes, and μ is the mobility. Since p is equal to $x-2y$, eq. (6) can be combined with eq. (8) to yield

$$\sigma = (e\mu P^{1/2}_{O_2}/4K)[(8xKP^{-1/2}_{O_2} + 1)^{1/2} - 1] . \quad (9)$$

In the high P_{O_2} region, $[V_O^{\cdot\cdot}] = 0$, and the hole concentration is dominated by the concentration of Ca. Thus, $y=0$, $p=x$ and eq. (9) reduces to

$$\sigma = e\mu x . \quad (10)$$

For the low P_{O_2} region, the oxygen vacancy concentration provides a significant compensation for the Ca dopant, and the concentration of holes will be reduced. In this region, the term $8xKP^{-1/2}_{O_2} \gg 1$, and the neutrality condition becomes $p = [Ca^{\prime}] - 2[V_O^{\cdot\cdot}]$. Eq. (9) will then reduce to

$$\sigma' = e\mu' (x/2K)^{1/2} P^{1/4}_{O_2} . \quad (11)$$

Therefore, σ' will have a $P^{1/4}_{O_2}$ dependence after the electrical compensation changes from electronic to ionic, provided that the mobilities in both regions are assumed to be nearly equal ($\mu = \mu'$), i.e., the mobility is independent of oxygen concentration. In this case

$$\sigma'/\sigma = P^{1/4}_{O_2} / (2Kx)^{1/2} . \quad (12)$$

With this assumption, K can be evaluated from a plot of σ'/σ versus $P^{1/4}_{O_2}$.

3. Experimental

Ca-doped $YCrO_3$ powders were synthesized using a modified liquid mix technique [16]. Compositions of 5, 10, 15, and 20 at% Ca in $YCrO_3$ were prepared. The Ca ions occupy the Y site ($Y_{1-x}Ca_xCrO_3$). Carbonates and nitrates were completely dissolved into solutions of ethylene glycol, citric acid, nitric acid and de-ionized water. The solutions were then slowly evaporated at 150°C without forming precipitates. Further decomposition of

the resulting organics occurred at 400°C. In order to completely pyrolize the remaining organics and form the oxides, all samples were calcined at 950°C for 12 h. This yielded fine-grained (~ 1 μm), homogeneous powders of the desired composition. X-ray diffraction analysis confirmed the absence of any measurable secondary phases, suggesting complete solid solution of the dopants into the compounds.

Electrical conductivity and Seebeck samples were formed by dry pressing at 7000 kg/cm^2 and then sintering the compacts at approximately 1750°C and 10^{-10} atm for 24 h, followed by annealing in air at 1550°C for 48 h. Bulk densities of about 96% of theoretical (5.55 gm/cc) were obtained. Rectangular specimens, usually $3\times3\times12$ mm^3, were cut from the annealing discs. To reduce the effects of barrier layers and nonohmic contacts, Pt paste was applied to the contact faces of the specimens.

Four-wire dc electrical conductivity and Seebeck measurements were performed using a computer-controlled apparatus that has been described in detail elsewhere [17]. The specimen was held between two Pt blocks in an alumina lined specimen holder. Two type-S thermocouples (Pt versus Pt–10% Rh) were employed to monitor the temperature, one at each end of the specimen. The furnace atmosphere was controlled by flowing gas mixtures of N_2–O_2 or CO_2-forming gas at a linear flow rate of 0.5 cm/s. Oxygen activities were determined directly from thermodynamic calculations using the known flow ratios. These calculations were verified by pre- and post-sampling the gas mixtures using a Y_2O_3 stabilized ZrO_2 oxygen sensor maintained at 1000°C. The Seebeck coefficient was determined by applying a 25–30°C temperature gradient along the length of the specimen and measuring the temperature difference and then the EMF through the common leads of the thermocouples. Seebeck values were corrected for the thermoelectric power of Pt [18]. The electrical conductivity was determined using a 4-wire, two point contact Kelvin technique. Data acquisition campaigns of 8 to 10 days for each sample consisted of conductivity and Seebeck data retrieval at three different isotherms (1000, 1100, and 1200°C) as a function of oxygen activity. Checks for reversibility were made in all cases.

4. Results and discussion

4.1. Temperature dependence

Previous investigations have suggested that Ca-doped $YCrO_3$ [7] and several of the La perovskites ($LaFeO_3$ [19], $LaCrO_3$ [8,9], and $LaCoO_3$ [20]) conduct electricity via the small polaron hopping process. In order to confirm that this conduction mechanism is active in (Y, Ca)CrO_3 a number of criteria must be satisfied. It is known that the mobility of a small polaron is strongly affected by the lattice distortion associated with the charge carrier. Karim and Aldred [9] state that a conduction process can occur by a thermally activated small polaron hopping transport provided that the number of charge carriers is constant or slowly varying, but the mobility is exponentially dependent on temperature. For an adiabatic small polaron hopping mechanism, Goodenough [21,22] has expressed the mobility as

$$\mu=(1-x)(ea^2\nu_o/kT)\exp[-E_m/kT]\,, \qquad (13)$$

where x is the fraction of sites occupied, e is the unit charge, a is the intersite distance, ν_o is the optical phonon frequency, E_m is the mobility activation energy, k is the Boltzman constant, and T is the absolute temperature. If adiabatic small polaron hopping is suspected to be the principle conduction mechanism, then a plot of $\log \mu T$ versus $1/T$ should yield a straight line whose slope is proportional to the activation energy. Many investigators consider this activated character to be the main identifying aspect of small polaron conduction [9,23,24]. Because of the strong lattice to carrier interaction, the magnitude of the mobility would be expected to be relatively low. Goodenough suggested an upper limit of the mobility to be 0.1 cm^2/V s for small polarons.

It is expected that the charge carrier concentration should remain constant with temperature for a thermally activated mobility. It is known that the sign and magnitude of the Seebeck coefficient can be useful in determining the type and concentration of charge carriers. For the constant carrier density, degenerate energy state, small polaron hopping mechanism, the expression for the Seebeck coefficient Q, was derived by Heikes [25] to be

$$Q=\pm(k/e)[\ln((1-x)/x)+\Delta S'/k]\,, \qquad (14)$$

where k/e has the usual meaning, x is the fraction of hopping sites occupied and $\Delta S'$ is the vibrational entropy associated with the local distortions around the polaron. The plus and minus sign refer to hole and electron carriers respectively. In this case, small polaron hopping should lead to a temperature-independent Seebeck coefficient. Therefore, the Seebeck coefficient of a polaronic, acceptor doped, p-type semiconductor would be expected to decrease with increasing dopant concentration. The dimensionless $\Delta S'/k$ term, which according to Austin and Mott [26] is approximately equal to 0.1–0.2, is usually neglected. Goodenough [27] points out that the $\Delta S'/k$ term normally contributes less than 10 μV/K to Q and can be ignored in cases where the absolute value of the Seebeck coefficient is relatively large. He also states that the magnitude of the Seebeck coefficient should exceed 100 μV/K for small polaron conductors. If this is true, then the entropy term can be regarded as insignificant and the small polarons as non-interacting.

In a broad band semiconductor, conduction occurs by thermal activation of carriers from the donor level into the conduction band (n-type), or the acceptor level into the valence band (p-type), and their subsequent transport within the band. If the electrical conductivity can be attributed to a single type of charge carrier where a broad band conduction mechanism predominates, the Seebeck coefficient is then given by [26]

$$Q = \pm (k/e)[(\Delta E/kT) + A] , \tag{15}$$

where ΔE is the energy difference from the Fermi level to the transport level, and A is a dimensionless transport constant which can be 0–4 depending on the type of scattering mechanism. Compared to Heikes formula, this equation predicts a Seebeck coefficient that is strongly dependent on temperature. Therefore, a measurement of the Seebeck coefficient as a function of temperature can serve as a stringent test for small polaron transport.

If a temperature-independent Seebeck coefficient (carrier concentration) and thermally activated mobility are expected for the small polaron model, then according to eq. (8), a thermally activated electrical conductivity should also result. In this case, the electrical conductivity σ can be expressed as [28–31]:

$$\sigma = (A'/T) \exp(-E_c/kT) , \tag{16}$$

where A' is both a charge carrier and material dependent constant, and E_c is the activation energy for hopping conduction. Similar to the mobility, a plot of $\log \sigma T$ versus $1/T$ should yield a straight line whose slope is proportional to the activation energy, provided the adiabatic case is valid.

Direct current electrical conductivity measurements were performed on Ca-doped $YCrO_3$ in oxygen over a temperature range of 25 to 1200°C. Fig. 1 is a $\log \sigma T$ versus $1/T$ plot of these data. The linear behavior observed for each composition is consistent with the adiabatic small polaron model expressed by eq. (16). Activation energies (E_c) were calculated as 0.17 ± 0.01, 0.18 ± 0.01, 0.18 ± 0.01, and 0.18 ± 0.01 eV for 5 at%, 10 at%, 15 at%, and 20 at% Ca-doped $YCrO_3$, respectively. Both the magnitude and activation energies of the electrical conductivity were in good agreement with those of Weber et al. [7], where $E_c = 0.20$ eV for Ca-doped $YCrO_3$ was reported. In comparison, the activation energies for the $(La, Sr)CrO_3$ system were reported by Karim and Aldred [9] to vary from 0.11 to 0.19 eV.

Seebeck measurements were made on Ca-doped $YCrO_3$ in oxygen over a temperature range from 300 to 1200°C. A plot of the Seebeck coefficient versus temperature is shown in fig. 2. It was found that the sign of the Seebeck coefficient was positive for all compositions, which would indicate a p-type conduction process. The magnitude of the Seebeck coefficients for all compositions were in excess of 100 μV/K which is consistent with Goodenough's criterion for low concentrations of small polarons. The nearly temperature independent behavior and proportional decrease of Q with Ca dopant appears to support the small polaron model proposed by Heikes. To test the applicability of the Heikes equation, the average Seebeck coefficient for each dopant concentration was plotted as a function of $\ln[(1-x)/x]$ as shown in fig. 3. An experimental value of Boltzman's constant k, was calculated from the slope using the least squares method. The $\Delta S'/k$ term in eq. (14) was not expected to contribute significantly to the analysis and was excluded. The experimental value $k_c = 7.18 \times 10^{-5}$ eV/K was found to agree within 17% of the accepted theoretical value of 8.62×10^{-5} eV/K.

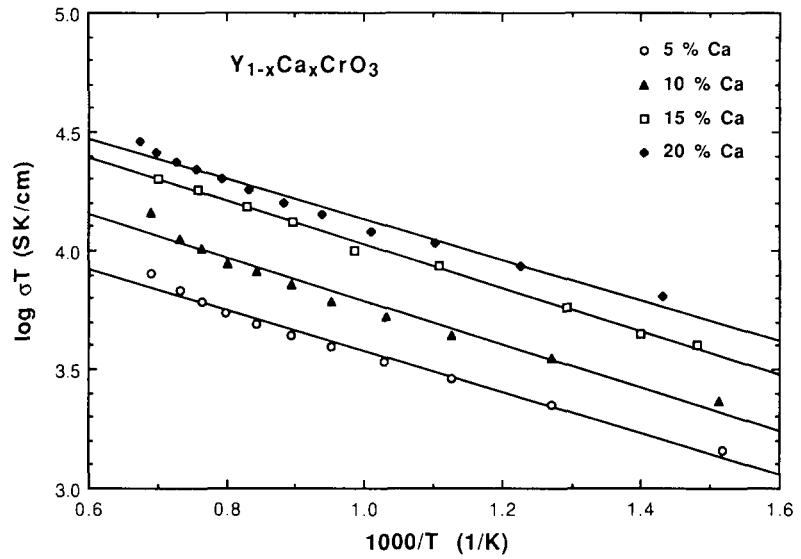

Fig. 1. log σT versus reciprocal temperature for Ca-doped $YCrO_3$.

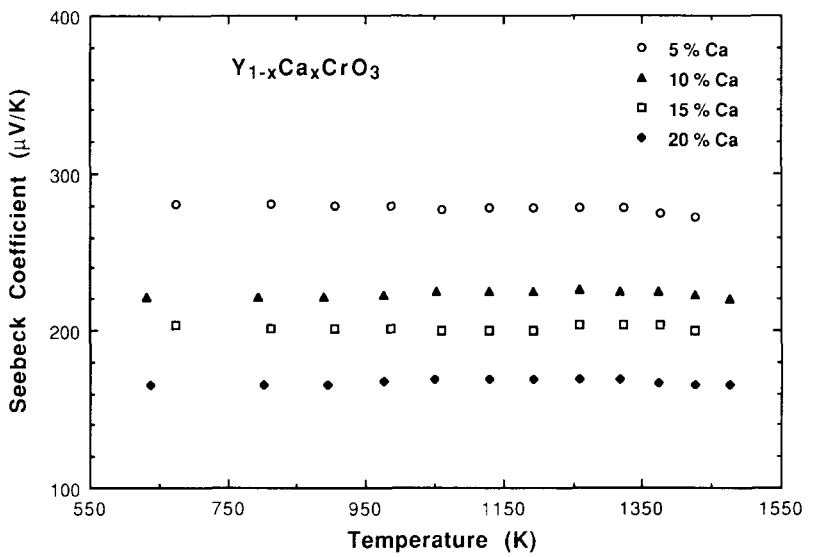

Fig. 2. Seebeck coefficient versus temperature as a function of Ca content in $YCrO_3$.

The mobilities in this study were determined by combining the Seebeck and electrical conductivity data. The electrical conductivity for hole conduction is represented by [13,19]

$$\sigma = (A_v/V_m)pe\mu\,, \qquad (17)$$

where A_v is Avogadro's number, V_m is the molar volume, p is the molar fraction of holes per mole of $Y_{1-x}Ca_xCrO_3$, and μ is the hole mobility. The Seebeck coefficient for holes (from eq. (14)) can be represented by

$$Q = (k/e)[\ln(N_V V_m/A_v P)]\,, \qquad (18)$$

where N_v is the density of states. It should be noted that the entropy term $\Delta S'/k$ was neglected and that the states were assumed nondegenerate. By combin-

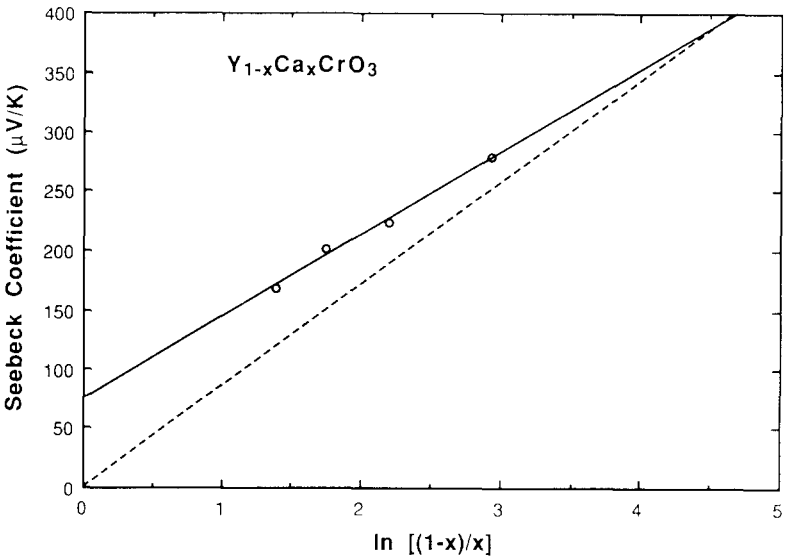

Fig. 3. Seebeck coefficient versus $\ln[(1-x)/x]$ for Ca-doped $YCrO_3$. The dashed line displays the theoretical slope.

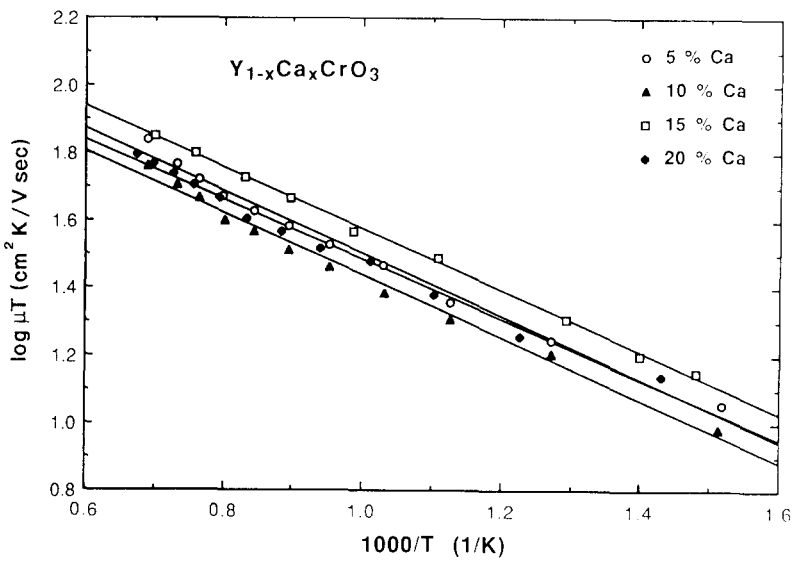

Fig. 4. $\log \mu T$ versus reciprocal temperature for Ca-doped $YCrO_3$.

ing eqs. (17) and (18), and solving directly for μ, the mobility becomes

$$\mu = (\sigma/N_v e)\exp(Qe/k)\,. \qquad (19)$$

Using the lattice parameters taken from ref. [7], the density of states N_v was calculated to be 1.84×10^{22} cm^{-3}. Fig. 4 is a $\log \mu T$ versus $1/T$ plot of the mobility data for Ca-doped $YCrO_3$. The mobilities were calculated from eq. (19) using the Seebeck coefficient and electrical conductivity values from figs. 1 and 2. The linear behavior observed is consistent with the argument for small polarons. Due to the nearly temperature independent Seebeck coefficient, the activation energy for conduction may be interpreted as the mobility activation energy [9]. Activation energies calculated from fig. 4 were identical to the

activation energies for conduction ($E_m = E_c$). Fig. 5 is a plot of electrical conductivity versus the Ca dopant concentration for various temperatures at 1 atm. If $[V_O^{\cdot\cdot}] = 0$ then the concentration of holes is equal to the Ca dopant concentration. An average value of the mobility can be calculated from the slope of the plot (fig. 5) and eq. (8). The calculated mobilities from this method were on the order of 0.03 cm^2/V s which compared well with mobilities calculated from eq. (19), which varied between 0.03 and 0.05 cm^2/V s for the same temperature range. The magnitude of the calculated mobilities fall below the upper limit of 0.1 cm^2/V s set by Goodenough for small polarons. The low values of μ indicate a high degree of localization by the charge carriers, which is an important characteristic of small polaron transport. Optical phonon frequencies ν_o, were calculated from the mobility data using eq. (13). The magnitude of ν_o for Ca-doped $YCrO_3$ was on the order of 1.3×10^{13} Hz which is reasonable for adiabatic small polarons [9].

From the above results, it would appear that Ca-doped $YCrO_3$ exhibits the characteristics of *p*-type conduction by hopping. The thermally activated behavior of the electrical conductivity and carrier mobility and the temperature independence of the Seebeck coefficient present strong evidence for the small polaron model. The good agreement between the conductivity and mobility activation energies for Ca-doped $YCrO_3$ follows from the temperature independence of the measured Seebeck coefficients. The magnitudes of the Seebeck coefficient and carrier mobility were compatible with Goodenough's criteria for small polaron hopping conduction. It is therefore concluded that Ca-doped $YCrO_3$ can be considered a good example of an adiabatic small polaronic conductor.

4.2. Oxygen activity dependence

dc electrical conductivity measurements, for Ca-doped $YCrO_3$, were made as a function of oxygen activity at 1000, 1100 and 1200°C. Typical results are displayed in fig. 6. The electrical conductivity was found to be independent of oxygen activity in the high P_{O_2} region. However, as the reduction progressed, the conductivity decreased as a function of P_{O_2} to the one quarter power. This behavior appears to be in full agreement with the expectations predicted by the model. The solid lines in fig. 6 were obtained from eq. (9) using the equilibrium constants calculated from eq. (12). Each line is a prediction from the model and represents the best fit solution of the respective data set to the equilibrium expression, eq.

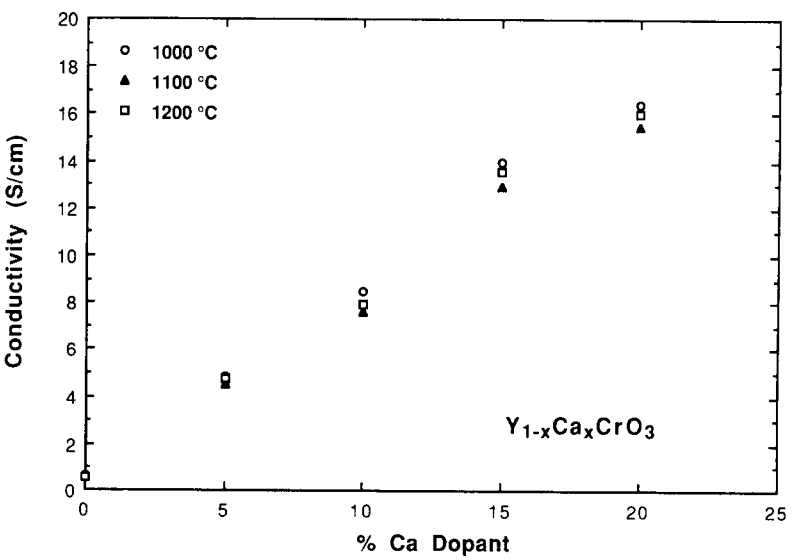

Fig. 5. Conductivity versus Ca-dopant concentration at various temperatures.

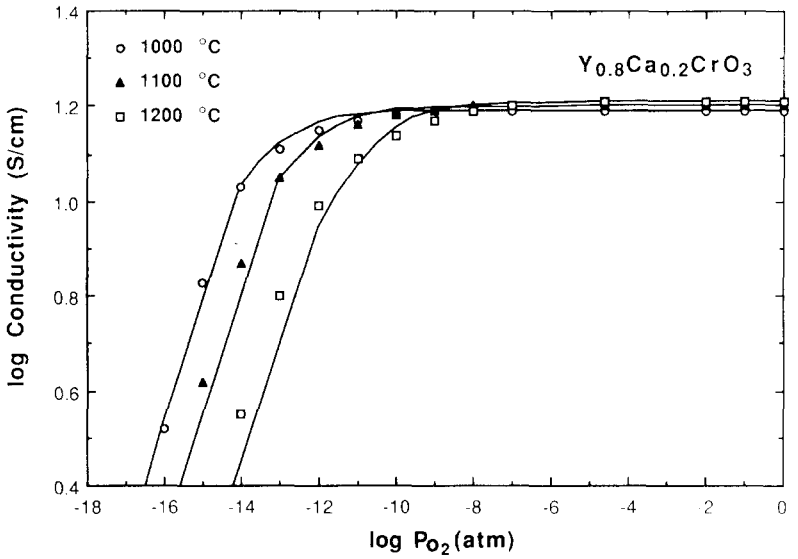

Fig. 6. Log conductivity versus log P_{O_2} for $Y_{0.8}Ca_{0.2}CrO_3$ at various temperatures.

(9). The fit between the model and the observed data is good (within 10%); however a small deviation exists at the "transition knee", which is the inflection located between the high and low P_{O_2} regions. This maybe due to defect clustering or complex formations that are assumed to be negligible in eq. (3) [32]. Although the model is oversimplified by assuming dilute solution conditions, it nevertheless describes the overall behavior quite well.

For the high P_{O_2} region, the carrier concentration is controlled by the acceptor content ($p=[Ca']$) and electronic compensation predominates. Any temperature dependence of the electrical conductivity is therefore determined by the mobility. It can be seen from the plots that the conductivity increases proportionally with both dopant concentration and temperature as predicted by eqs. (10) and (17). In the low P_{O_2} region, oxygen vacancies compensate for the Ca ions present ($p=[Ca']-2[V_O^{\cdot\cdot}]$) and a decrease in the electrical conductivity is observed. This is verified by the P_{O_2} dependence of the Seebeck coefficient as shown in fig. 7. In this case, the Seebeck coefficient is inversely dependent on the carrier concentration. In accord with the electrical conductivity, the Seebeck coefficient remains constant until the low P_{O_2} region is reached. At this point, the Seebeck coefficient rapidly increases at the transition knee because of its inverse relation with the carrier concentration. In agreement with eq. (12), the location of the transition knee shifted to a higher P_{O_2} with increasing dopant concentration and temperature in both the Seebeck and electrical conductivity data. It should be noted that in eq. (12), the mobility was assumed to be independent of oxygen activity. This is an important feature of the model if the calculated equilibrium constants are to be regarded as correct. To validate this assumption, the mobility as a function of P_{O_2} was determined by combining the electrical conductivity data in fig. 6 with the Seebeck data found in fig. 7 and eq. (19). Typical results of the calculated mobilities for Ca-doped $YCrO_3$ can be found in fig. 8. Although the uncertainty in the Seebeck ($\pm 6\%$), electrical conductivity ($\pm 2\%$), and the log P_{O_2} measurements (± 0.2) may seem small, they translate to uncertainty in the mobility as high as ± 0.01 cm^2/V s in the high P_{O_2} region and as high as ± 0.02 cm^2/V s in the low P_{O_2} region. Within this error range, the mobilities exhibited in fig. 8 can be considered independent of oxygen activity.

Table 1 lists the equilibrium constants derived from the electrical conductivity data and the associated thermodynamic parameters. The equilibrium constants from this study are very similar to those

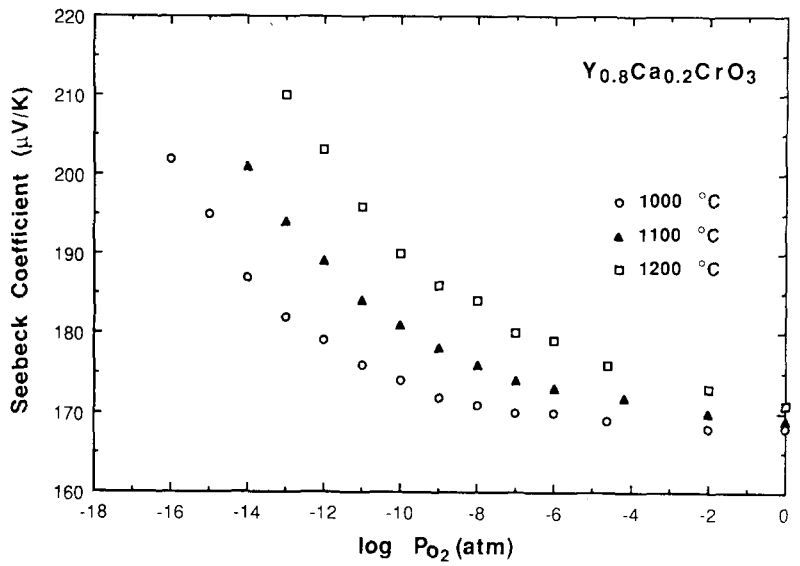

Fig. 7. Seebeck coefficient versus log P_{O_2} for $Y_{0.8}Ca_{0.2}CrO_3$ at various temperatures.

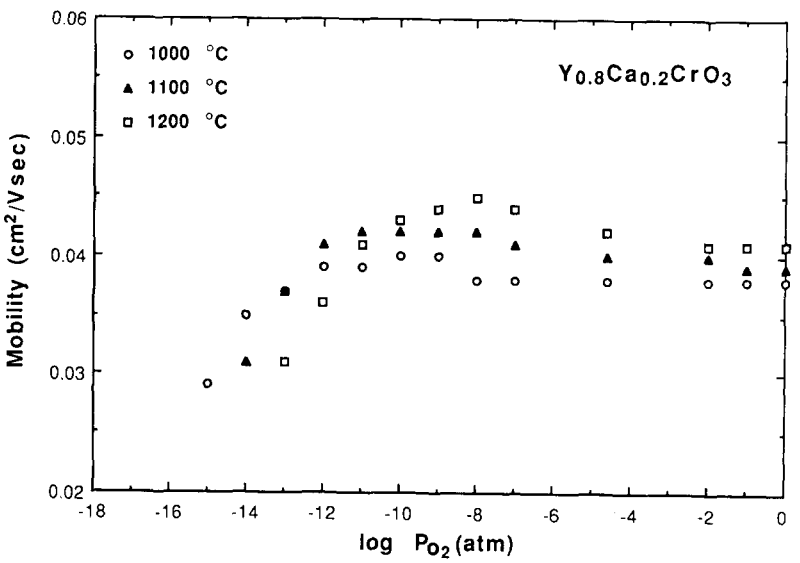

Fig. 8. Mobility versus log P_{O_2} for $Y_{0.8}Ca_{0.2}CrO_3$ at various temperatures.

derived by Flandermeyer et al. [33] for Mg-doped $LaCrO_3$. Fig. 9 is an Arrhenius plot of log K versus $1/T$ for the 5, 10, 15 and 20 at% Ca-doped specimens. The linear behavior and similar slopes exhibited by all of the compositions suggest that the free energies of formation are relatively constant with Ca dopant. The thermodynamic parameters, the partial molar enthalpy of formation of oxygen vacancies ΔH, and the partial molar entropy ΔS, were calculated from this plot using the following equations:

$$K = \exp(-\Delta G/RT) \tag{20}$$

and

Table 1
Table of thermodynamic values for $Y_{1-x}Ca_xCrO_3$.

Ca (at%)	$E_c = E_m$ (eV)	Temp. (°C)	Log K	
5	0.17	1000	−6.85	
		1100	−6.31	$\Delta H = 189 \pm 15$ kJ/mole
		1200	−5.79	$\Delta S = 18$ J/mole K
10	018	1000	−6.66	
		1100	−6.14	$\Delta H = 196 \pm 15$ kJ/mole
		1200	−5.57	$\Delta S = 25$ J/mole K
15	0.18	1000	−6.48	
		1100	−5.98	$\Delta H = 203 \pm 15$ kJ/mole
		1200	−5.34	$\Delta S = 35$ J/mole K
20	0.18	1000	−6.29	
		1100	−5.81	$\Delta H = 242 \pm 18$ kJ/mole
		1200	−5.11	$\Delta S = 67$ J/mole K

$$\Delta H = \Delta G + T\Delta S\,, \tag{21}$$

where ΔG is the Gibbs free energy, R is the gas constant, and T is the absolute temperature. It is interesting to note that eqs. (4) and (20) predict an increase in the oxygen vacancy concentration with increasing temperature at a given P_{O_2}. This observation was consistent with the trends found in the data and the model. It is therefore evident that both temperature and Ca content have a profound influence on the P_{O_2} range over which the electrical conductivity and Seebeck coefficient can be expected to be invariant. A composite expression for the equilibrium constant given by eqs. (4) and (20) for Ca-doped $YCrO_3$ was calculated to be

$$K = (92.1)\exp(-\Delta H/RT)\,, \tag{22}$$

where $\Delta H = 208 \pm 16$ KJ/mole which, from eq. (3), is the enthalpy of formation of oxygen vacancies. This is comparable with Flandermeyer's value of 272 ± 16 KJ/mole for Mg-doped $LaCrO_3$ [33,34].

5. Conclusions

Ca-doped $YCrO_3$ showed p-type electrical conductivity and high stability towards reduction. The data obtained from the electrical conductivity experiments support the proposed defect model for the oxidation-reduction behavior. In the high P_{O_2} region, the conductivity is controlled by Ca content with little P_{O_2} dependence, at low P_{O_2}, the conductivity is controlled by the formation of $[V_O^{\cdot\cdot}]$ and has an approximate 1/4 power dependence on P_{O_2}. The P_{O_2} at which the conductivity starts to decrease (transition "knee") increases with the increase of either temperature or Ca content. Mobilities were calculated by the combination of Seebeck and conductivity data and were found to be very small (003–

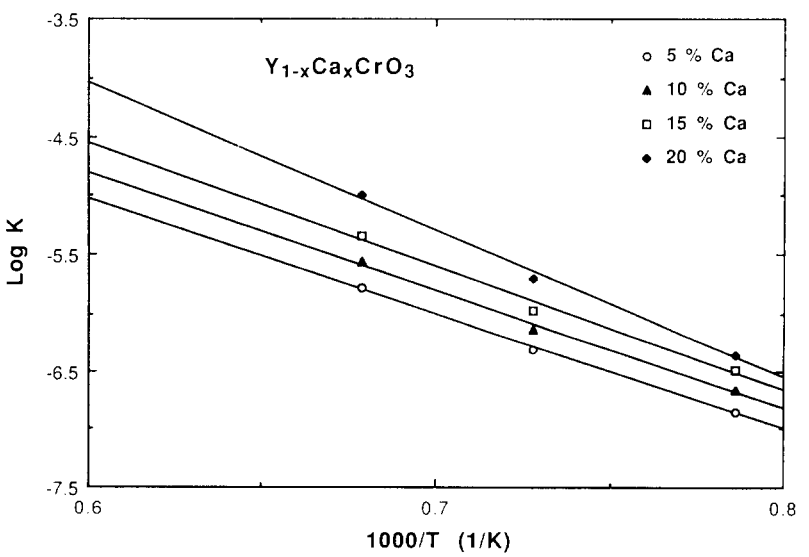

Fig. 9. Plot of log equilibrium constant versus reciprocal temperature for Ca-doped $YCrO_3$.

0.05 cm^2/V s) indicating a localized nature for the charge carriers. Analysis of the data suggest that conduction occurs via the small polaron hopping process.

Acknowledgement

This research was supported by the United States Department of Energy, Basic Energy Science Division and Morgantown Energy Technology Center.

References

[1] W. Feduska and A.O. Isenburg, J. Power Sources 10 (1983) 89.
[2] H.U. Anderson, R. Murphy, K. Humphrey, B. Rossing, A.J. Aldred, W.L. Procarione and R.J. Ackermann, Conf. High Temperature Sciences Related to Open Cycle, Coal-Fired MHD Systems (Argonne Natl. Lab., April, 1977).
[3] H.K. Bowen, J.W. Halloran and W.T. Petuskey, in: Corrosion Problems in Energy Conversion and Generation, ed. C.S. Tedmon Jr. (The Electrochem. Soc., New York, 1974).
[4] H.K. Bowen and B.R. Rossing, Materials Limiting Problems in Energy Production (Plenum, New York, 1976).
[5] D.B. Meadowcroft, Brit. J. Appl. Phys. 2 (1969) 1225.
[6] W.J. Weber, J.L. Bates, C.W. Griffin and L.C. Olsen, in: Defect Properties and Processing of High-Technology Nonmetallic Materials, eds. Y. Chen, W.D. Kingery and R.J. Stokes (Mat. Res. Soc., Pittsburgh, PA, 1986) pp. 235–242.
[7] W.J. Weber, C.W. Griffin and J.L. Bates, J. Am. Ceram. Soc. 70 (1987) 265.
[8] J.B. Webb, M. Sayer and A. Mansingh, Can. J. Phys. 55 (1977) 1725.
[9] D.P. Karim and A.T. Aldred, Phys. Rev. B 20 (1979) 2255.
[10] T. Negas and W.R. Hosler, in: Energy and Ceramics, ed. P. Vincenzini (Elsevier, New York, 1980).
[11] H.U. Anderson, M.M. Nasrallah, B.K. Flandermeyer and A.K. Agarwal, J. Solid State Chem. 56 (1985) 325.
[12] J.H. Kuo, H.U. Anderson and D.M. Sparlin, J. Solid State Chem. 83 (1989) 52.
[13] J.H. Kuo, H.U. Anderson and D.M. Sparlin, J. Solid State Chem. 87 (1990) 55.
[14] R.F. Huang, H.U. Anderson and A.K. Agarwal, J. Am. Ceram. Soc. 67 (1984) 146.
[15] F.A. Kröger and H.J. Vink, Solid State Physics, eds. F. Seitz and D. Turnbull, Vol. 3 (Academic Press, New York, 1956).
[16] M. Pechini, U.S. Pat. 3,330,597, 1967.
[17] G.F. Carini II, M.Sc. Thesis (University of Missouri-Rolla, 1987).
[18] N. Cusak and P. Kendall, Proc. Phys. Soc. 72 (1985) 5.
[19] J. Mizusaki, T. Sasamoto, W.R. Cannon and H.K. Bowen, J. Am. Ceram. Soc. 66 (1983) 247.
[20] P. Dordor, S. Joiret, J.P. Donmerc, J.C. Launay, J. Claverie and P. Hagenmuller, Phys. Status Solidi a 93 (1986) 321.
[21] J.B. Goodenough, J. Appl. Phys. 37 (1966) 1415.
[22] J.B. Goodenough, Phys. Rev. 164 (1967) 785.
[23] H.L. Tuller and A.S. Nowick, J. Phys. Chem. Solids 38 (1977) 859.
[24] N.F. Mott and E.A. Davis, Electronic Processes in Noncrystalline Materials (Clarendon, Oxford, 1971).
[25] R.R. Heikes, in: Thermoelectricity, eds. R. Heikes and R. Ure (Interscience, New York, 1961).
[26] G. Austin and N.F. Mott, Adv. Phys. 18 (1969) 41.
[27] J.B. Goodenough, Mat. Res. Bull. 5 (1970) 621.
[28] A.J. Bosman and H.J. Van Dal, Adv. Phys. 19 (1970) 1.
[29] J.B. Goodenough, Metallic Oxides,in: Progress in Solid State Chemistry, ed. H. Reiss, Vol. 5 (Pergamon Press, New York, 1971).
[30] J.M. Wimmer and I. Bransky, in: Electronic Conduction, Electrical Conductivity in Ceramics and Glass, ed. N.M. Tallan (Marcel Dekker, New York, 1974) p. 290.
[31] R.R. Heikes, in: Thermoelectricity: Science and Engineering, eds. R.R. Heikes and R.W. Ure (Wiley–Interscience, New York, 1961).
[32] O.T. Sørensen, Nonstoichiometric Oxides (Academic Press, New York, 1981).
[33] B.K. Flandermeyer, M.M. Nasrallah, A.K. Agarwal and H.U. Anderson, J. Am. Ceram Soc. 67 (1984) 195.
[34] B.K. Flandermeyer, M.M. Nasrallah,, D.M. Sparlin and H.U. Anderson, High Temp. Sci. 20 (1985) 259.